

Journal Pre-proofs

Research paper

Buffer Gas Cooling for Sensitive Rotational Spectroscopy of Ice Chemistry: A Proposal

Ranil M. Gurusinghe, Nureshan Dias, Bernadette M. Broderick

PII: S0009-2614(20)31037-X
DOI: <https://doi.org/10.1016/j.cplett.2020.138125>
Reference: CPLETT 138125

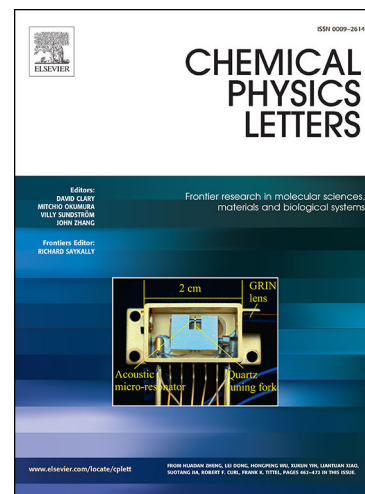
To appear in: *Chemical Physics Letters*

Received Date: 4 August 2020
Revised Date: 25 September 2020
Accepted Date: 21 October 2020

Please cite this article as: R.M. Gurusinghe, N. Dias, B.M. Broderick, Buffer Gas Cooling for Sensitive Rotational Spectroscopy of Ice Chemistry: A Proposal, *Chemical Physics Letters* (2020), doi: <https://doi.org/10.1016/j.cplett.2020.138125>

This is a PDF file of an article that has undergone enhancements after acceptance, such as the addition of a cover page and metadata, and formatting for readability, but it is not yet the definitive version of record. This version will undergo additional copyediting, typesetting and review before it is published in its final form, but we are providing this version to give early visibility of the article. Please note that, during the production process, errors may be discovered which could affect the content, and all legal disclaimers that apply to the journal pertain.

© 2020 Published by Elsevier B.V.



Buffer Gas Cooling for Sensitive Rotational Spectroscopy of Ice Chemistry: A Proposal

Ranil M. Gurusinghe, Nureshan Dias, **Bernadette M. Broderick***

University of Missouri, Department of Chemistry, Columbia, Missouri, USA

Keywords: broadband rotational spectroscopy, buffer gas cooling, interstellar ice chemistry

Abstract

High temperatures and associated poor rotational partition functions have hindered the application of high-resolution rotational spectroscopy for detection of molecules desorbing from an ice substrate. Here, an experimental approach is presented which will enable such investigations through incorporation of a buffer gas cooling cell. We discuss design considerations for this apparatus and the expected performance based upon OC³⁴S measurements made with a related spectrometer in a 14.7 K sampled uniform flow. We highlight specific applications of this technique including chiral sensing of molecules generated in an interstellar ice, and the synthesis of exotic species not amenable to generation in the gas-phase.

*Correspondence to: broderickbm@missouri.edu

I. Introduction

Chemistry taking place in ices profoundly impacts atmospheric chemistry and chemistry in astrochemical environments[1,2]. For example, the synthesis of prebiotic amino acids and sugars, as well as the enantiomeric excess observed on Earth may be attributed to chemistry that took place in ice[3,4]. However, current laboratory studies mainly employ mass spectrometric and Fourier-transform infrared spectroscopic detection and do not take advantage of recent tremendous advances of broadband rotational spectroscopy[5,6]. This is largely because of the disadvantage of the rotational partition function associated with molecules desorbing from these ices at typical temperatures from 80-200 K. A means to cool these molecules offers the advantage of rotational spectroscopy for effective probes of chirality, isomer-specificity, complex mixture analysis, and meaningful relative intensities for product branching ratios.

There have been, to our knowledge, two reports on the application of millimeter and submillimeter spectroscopy applied to study interstellar ice chemistry. Widicus-Weaver et al. demonstrated the first such experiments in their detection of thermally desorbed H₂O, D₂O, and CH₃OH originating in a solid film created at ~ 12K[7]. Ultimately, the thermodynamic values ΔH and ΔS were derived, and the surface binding energy of H₂O was measured and found to be consistent with previous reports. The apparatus in that work employed a high-vacuum chamber within which ices are generated. Following temperature-programmed desorption (TPD), molecules entering the gas-phase were irradiated with a mm/submm radiation source, and detected with a cryo-cooled THz hot-electron bolometer. The limit of detection (LOD) which reflects the lowest gas density at which a S/N ratio of 3 can be achieved on a single rotational transition was determined to be 1.1×10^9 molecules cm⁻³ for the $1_{1,0} \leftarrow 1_{0,1}$ rotational transition of H₂O. Similarly, the LOD for the $1_{1,1} \leftarrow 0_{0,0}$ transition of D₂O and $13_{-1,13} \leftarrow 12_{-1,12}$ transition of CH₃OH were determined to be 1.7×10^9 molecules cm⁻³ and 3.1×10^{10} molecules cm⁻³ respectively.

The second application of rotational spectroscopy to interrogate molecules subliming off of an ice surface was recently reported by Potapov et al[8]. In contrast to the initial work of Widicus-Weaver et al, this group employed broadband chirped-pulse Fourier-transform microwave (MW)

spectroscopy to interrogate NH_3 ice generated in a U-shaped waveguide at $\sim 20\text{K}$ under high-vacuum conditions. Following deposition of several ice monolayers within the waveguide, TPD experiments were performed and the MW inversion spectrum of the NH_3 (J,K) = (1,1), (2,2), (3,3) and (4,4) transitions over 1 GHz was recorded. The E_{des} was reported and in reasonable agreement with previously reported FTIR data. The sensitivity of this instrument was determined to be 3×10^{12} molecules in the 19.1 cm^3 of the waveguide, or about 5 pmol.

The proof-of-principle experiments above reveal the potential for rotational spectroscopy to provide important insight into the chemistry of interstellar ices. Here, we outline an alternative approach to probe molecules that have sublimed from a solid surface (such as an interstellar or cometary ice) via broadband rotational spectroscopy with greatly improved sensitivity by coupling an ultra-high vacuum ice instrument with a buffer gas cooling cell operating at 15 K.

Buffer gas cooling has proven to be an efficient, near-universal way in which to cool molecules[9-14], making it well-suited to couple with ice experiments. In such studies, ices are typically irradiated to induce chemistry, then warmed to sublime at temperatures exceeding 80 K, giving rise to a very unfavorable partition function for detection by rotational spectroscopy[15,16]. Buffer gas cooling can operate with small cells (a few cm^3) due to the cold elastic cross section of helium (or neon) with any molecule ($\sim 10^{-14} - 10^{-15} \text{ cm}^2$), allowing for straightforward incorporation into other systems or coupling with other techniques[17]. In addition, high densities of buffer gas are not required to achieve temperatures in the few kelvin regime. Cryo-pumps are typically employed in buffer gas cells; here, we suggest that a single turbomolecular pump will be adequate to achieve the necessary pressures for efficient buffer gas cooling in a machine that will generate ices under ultra-high vacuum conditions and provide added flexibility and reduced maintenance.

A number of detailed reviews on buffer gas cooling have been given[9,10,18] and only a brief description of the approach is included here. Buffer gas cooling typically involves a copper cell that is in thermal contact with a cryostat. Buffer gas atoms enter the cell with typical densities ranging from $\sim 10^{14} - 10^{17} \text{ cm}^{-3}$ which is high enough to thermalize the molecules of interest, and low enough to prevent cluster formation. The reactant molecules are introduced to the cell and

perform a random walk within it due to repeated elastic/inelastic collisions with the buffer gas atoms. Ultimately, these cooled molecules hit the cell walls at which time they freeze out and are lost. Both simulations and experiments indicate that under select conditions the thermalization process is substantially more rapid than diffusion.

The first application of the buffer gas cooling technique was by the De Lucia group who examined CO-He collisions at 4 K[19]. A number of subsequent experiments by this group and others have exploited the simple, general, and robust nature of the buffer gas cooling approach. Elegant experiments such as those by Patterson et al have achieved enantiomer-specific state transfer of chiral molecules based on microwave three-wave mixing within a buffer gas cell where high densities, continuous operation and high repetition rates for detection are achievable (~ 60 kHz)[20]. McCarthy and coworkers have demonstrated the ability to use buffer gas cooling as a powerful analytical tool for complex mixture analysis and trace species detection by high-resolution chirped-pulse Fourier-transform microwave spectroscopy[21,22]. Buffer gas cooling has enabled the study of chemical reactions at ultra-cold temperatures and has made precision measurements possible in the quantum regime[23,24].

In the approach described here, the primary purpose of the buffer gas cell is to cool molecules to $T \leq 20$ K in order to lower the rotational partition function allowing for sensitive detection of molecules subliming off of an ice surface. One of the chief applications of this technique is to enable the study of cosmic-ray driven chemistry in ices on grains with high-resolution rotational spectroscopy. We emphasize that the current approaches which apply rotational spectroscopy to interrogate ice chemistry can thus be improved by orders of magnitude simply by lowering the temperature of those molecules being probed, while still preserving the nascent distribution of molecules and without inducing any chemistry beyond that which took place within the ice. The paper is structured as follows: In Section II we sketch the instrument we envision to perform these studies and outline its design parameters; in Section III we consider the issues involved in buffer gas cooling of molecules desorbing from a surface and justify the choices made in the proposed design; in Section IV we use mmWave spectra recorded for known low densities of OC^{34}S at 14.7 K to estimate the signal to noise expected from the proposed instrument.

II. Apparatus

Figure 1 includes a sketch of the ultra-high vacuum (UHV) apparatus that we will employ to carry out this work. Ultra-high vacuum (10^{-11} torr) is achieved with a single high-throughput 2400 L/s magnetic bearing turbomolecular pump which is backed by an oil-free scroll pump. Two cold-heads reside within the chamber. Ices will first be generated by depositing gas-phase species such as water, methanol, carbon monoxide (both pure and mixed) to the 4 K 1 cm x 1 cm surface on cold-head 1 which is rotatable in the X-Z plane and translatable along the Y axis with UHV bellows, inspired by the W.M. Keck machine in the Kaiser group.[25] A series of windows surround the base of the machine to allow light, a keV electron gun, and other radiation sources to enter into the machine to characterize the ice and induce chemistry within it. Following this irradiation period, cold head 1 will be raised via the UHV bellows such that the 1 cm x 1 cm ice surface is positioned facing the entrance aperture of the buffer gas cell which is in thermal contact with cold head 2. The distance between the ice surface and the cell entry orifice is 0.5 cm. Temperature-programmed desorption (TPD) experiments will then be performed, during which time the ice molecules will enter into the gas phase. Given the experimental geometry of the ice surface with respect to the entry orifice and assuming molecular flow (discussed below), ~50% of the gas-phase molecules subliming from the ice will make it into the buffer gas cell to be cooled. A summary of the analysis performed to optimize this approach is given in Section III.

Broadband rotational spectroscopy will then be applied to interrogate molecules that have sublimed from the ice surface and have been cooled within the cell. Sapphire windows are mounted on both the buffer gas cell and main chamber to allow mm-wave radiation to pass through as the horns are located for convenience on the exterior of the machine. A receiver horn is located on the buffer gas cell itself followed by two low-noise amplifiers, waveguide, and final receiver horn. Following down-conversion, the time-domain free-induction decay signal is sent into a fast oscilloscope and Fourier-transformed to a frequency domain signal[6].

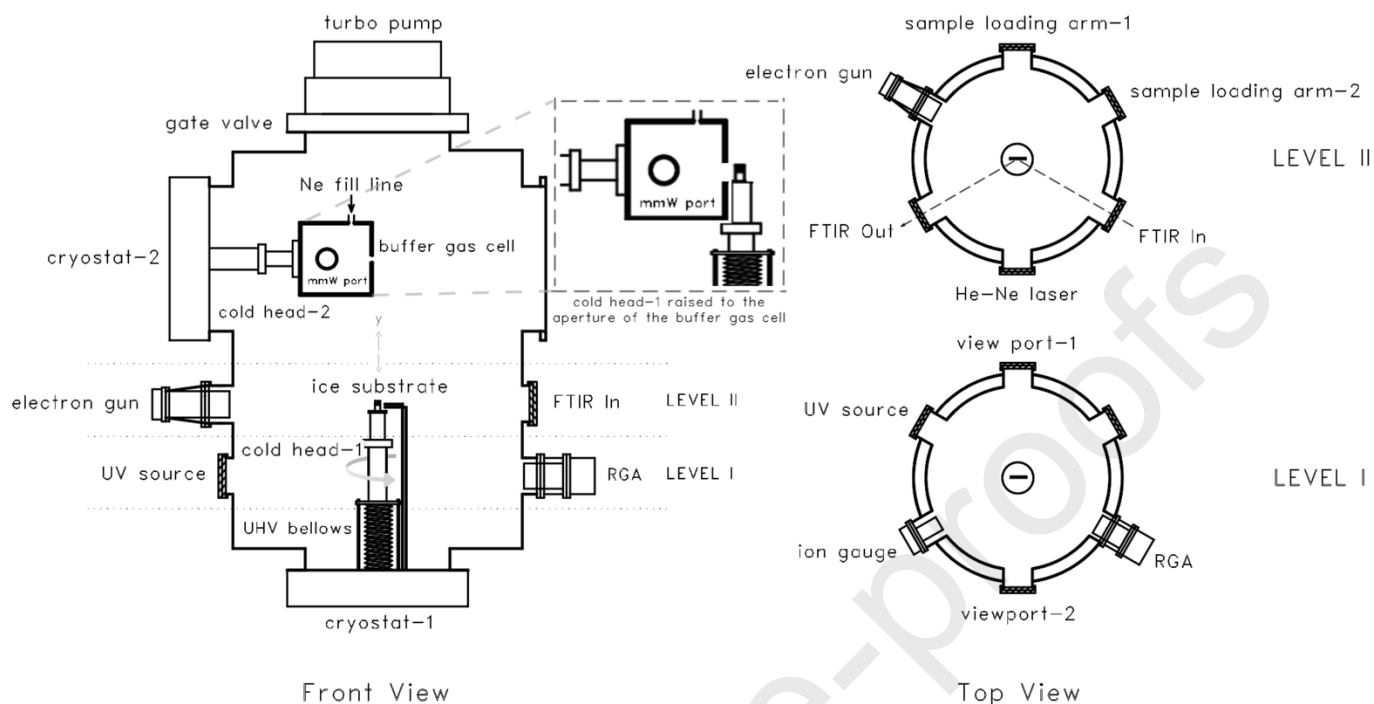


Figure 1. Schematic of the experimental apparatus to be employed in the proposed work.

III. Buffer gas cooling considerations

To optimize the buffer gas cooling for molecules subliming from an ice surface for detection by rotational spectroscopy, a number of factors must be considered in the experimental design. These are driven by the translational and rotational cooling times which should be much shorter than the diffusion time of the molecules in the cell, and the buffer gas volume flow rate and aperture area which together determine the buffer gas density and hence the diffusion and cooling times.

Buffer Gas Cell & Pumping Requirements

The buffer gas cell described here is similar to those previously reported[26,27], with two key differences to allow for a more straightforward coupling with laboratory ice experiments. First, almost all previous work performed in a buffer gas cell (not so with buffer gas-beams[14,28]) use helium as the buffer gas nominally at 4 K. The cell in the apparatus outlined here employs neon and is assumed to operate between 12-20 K. Secondly, all buffer gas cells employ charcoal-based cryogenic sorption pumps which are incompatible with UHV ice experiments.

We show below that a single high-throughput 2400 L/s turbomolecular pump can achieve the UHV conditions required for the generation of contaminant-free ices, as well as meet the pumping demands of a wide range of helium or neon flows within the cell.

Despite its limited use in buffer gas cooling, neon offers several technical advantages over helium as the buffer gas. First, radiation shielding is less critical in buffer gas cooling at 12-20 K. The blackbody heat load on a 4 K helium cell from a 300 K surface is $\sim 50 \text{ mW cm}^{-2}$ [10]. Buffer gas cells often have surface areas $> 100 \text{ cm}^2$ which would overwhelm the majority of cryogenic refrigerators due to additional heat loads, and as a result, cold radiation shielding is necessary when operating helium at 4 K in a cell. Neon, on the other hand, can achieve low temperatures (lower limit $\sim 12 \text{ K}$) with less stringent requirements on radiation shielding due to the higher operating temperature and increased heat load tolerances. For example, for a typical cryocooler with 50 W at 77 K on the first stage, one obtains greater than 15 W on the second stage at 15 K, but only 1.5 W at 4 K. This flexibility in radiation shielding also allows for greater conductance to the turbo pump, as well as a simpler interface between two cold-heads operating in a single vacuum chamber.

Diffusion and cooling times

In the following we consider both helium and neon as buffer gases but choose 7 K and 15 K, respectively, as the target temperatures. In order for buffer gas cooling to be effective, the diffusion time of molecules in the cell must greatly exceed the time it takes to cool the molecules. The number of collisions required for cooling can be estimated by equation 1 which assumes elastic collisions between two mass points, m (buffer gas atom) and M (target molecule), where $\kappa \equiv (M + m)^2/(2Mm)$, T' is the temperature of the molecules upon entering the cell, and T_l is the temperature of the atom or molecule after l collisions with the buffer gas atom[18].

$$\frac{T_l}{T} = \left(\frac{T'}{T-1}\right)e^{-l/\kappa} + 1 \quad \text{Eq. 1}$$

We initially assume a steady-state neon density of 1.9×10^{14} (see Table 1). Under the conditions of $T = 15$ K, $T' = 200$ K for molecules entering the gas-phase from the ice with $m = 60$ amu, roughly 13 collisions are required for the molecules to fall below 20 K (T) with neon as the buffer gas, corresponding to a cooling time of 0.3 ms. Although this refers to translational cooling, rotational cooling takes place on similar time scales[29]. For helium, 38 collisions are required to achieve 7 K from $T' = 200$ K, corresponding to 0.8 ms. A key metric is the cooling time relative to the total diffusion time that the molecules spend in the cell, or the fraction of their time in the cell that the molecules are at the target temperature or below. This diffusion time (i.e., before the molecules hit the cell wall and are lost), τ_{diff} , is given by[10]:

$$\tau_{diff} = \frac{A_{cell}16(n_{0,s} + n_{0,b})\sigma_{b-s}}{18} \sqrt{\frac{\mu}{2\pi k_B T_0}} \quad \text{Eq. 2}$$

where A_{cell} is the cross-sectional area of the buffer gas cell, $n_{0,b}$ is the stagnation number density of buffer gas atoms, and σ_{b-s} is the thermally averaged elastic collision cross section. In contrast to previous work, one cannot assume $m_s \gg m_b$ due to the heavier mass of neon in comparison with helium, and therefore Eq. 2 is used to determine the diffusion time here. For a 100 cm² cell, a n_{Ne} of 1.9×10^{14} mol · cm⁻³ (cell pressure $\sim 3.8 \times 10^{-4}$ torr), and σ_{b-s} of 2.4×10^{-15} cm², a diffusion time of ~ 1.8 ms is expected, so that 83% of the time spent in the cell, the molecules have reached the target temperature of 20 K. The case for helium at 7 K is slightly less favorable. The diffusion time for a similar buffer gas density (1.6×10^{14} mol · cm⁻³, 5 sccm helium flow, with a conductance through the aperture of 14.2 L/s and corresponding cell pressure of $\sim 1.1 \times 10^{-4}$ torr) is 1.6 ms, which suggests that the molecules of interest have reached the target temperature for 50% of the time in the cell before diffusing to the walls.

Buffer Gas Loading of Sublimed Molecules

To estimate the steady-state concentration of cold probed molecules within the cell, we determine their flow rate into the cell, the fraction that are cold as determined above, and the flow of buffer gas into and out of the cell. We first consider the flow rate of molecules subliming from the ice for detection within the buffer gas cell. As an example we consider a simple ice

composed of pure glycolaldehyde (CH_2OHCHO), an important precursor to the formation of RNA and the first extraterrestrial sugar detected in the ISM[30]. A sample $1\ \mu\text{m}$ thick over an area of $1\ \text{cm}^2$ contains a total of 1.2×10^{18} molecules. In order to maximize the number of molecules which enter the cell, the ice substrate is placed $0.5\ \text{cm}$ away from the entry orifice but thermally isolated from the cell. At this distance, we consider a $2\ \text{cm}$ diameter orifice ($\sim 3\ \text{cm}^2$) that will admit 50% of the molecules into the cell. Considering the cell entry region exclusively where the local pressure can be estimated to be $<10^{-4}$ torr, at $200\ \text{K}$ at which the glycolaldehyde will desorb, the mean free path is $> 3\ \text{m}$ so it is free molecular flow.

The steady-state composition of molecules within the cell is dependent upon several factors. We first consider the above scenario where 50% of the sublimed molecules from the glycolaldehyde ice enter the buffer gas cell over the course of a typical TPD experiment. In such an experiment, the substrate temperature is slowly ramped and the molecule of interest is liberated over the course of perhaps 5 minutes (although it can be much longer). There is thus a flow of $\sim 4 \times 10^{15}$ mol s^{-1} entering the cell. Pre-cooled buffer gas atoms are simultaneously introduced to the cell through a separate orifice, typically at flow rates ranging from $1 - 20$ sccm. We select 4 sccm as an initial flow rate, or 1.8×10^{18} atoms s^{-1} of neon, to achieve efficient cooling, long diffusion times and modest pumping demands. This suggests a concentration of $\sim 0.22\%$ of the sample molecules during their desorption time. In addition to entrance flow rate, the steady-state conditions within the cell are also determined by the conductance of the aperture through which the buffer gas atoms will exit. Under molecular flow conditions, the conductance, C , of the $3\ \text{cm}^2$ aperture is $9.2\ \text{L s}^{-1}$ as determined by Equation 3,

$$C (\text{L}\cdot\text{s}^{-1}) = 0.1A\sqrt{\frac{RT}{2\pi m}} \quad \text{Eq. 3}$$

where R is the universal gas constant, T is the thermodynamic temperature, m is the molar mass and A is the cell aperture area in cm^2 . The mean free path within the cell at $P = 3.8 \times 10^{-4}$ torr is $\sim 5\ \text{mm}$. Although strictly speaking this is transitional flow (Knudsen number 0.25), the conductance expression should be roughly valid as this condition is close to the molecular flow

regime. We can therefore neglect the interaction between the neon atoms coming out of the cell and the molecules that are desorbing from the ice.

Given an aperture conductance of 9.2 L s^{-1} and flow rate of 4 sccm, the steady-state number density of buffer gas atoms within the cell will be $1.9 \times 10^{14} \text{ atoms cm}^{-3}$; at the 0.22% concentration determined above this suggests 4.2×10^{11} target molecules within the cell, of which roughly 83% or 3.5×10^{11} will be at the desired temperature. This is well within the detection limits of the broadband spectrometer to be used in this work as demonstrated further below. We note that the number density of the molecule of interest is independent of the buffer gas atom flow rate; the latter governs the diffusion time and collision frequency which is adjusted accordingly to maximize the observed rotational spectroscopic signal. A range of densities can be achieved within the cell and how this relates to flow rate is summarized in Table 1.

Ne Buffer Gas Flow Rate, sccm	1	4	8	12	18
Buffer Gas Atoms, s^{-1}	4.5×10^{17}	1.8×10^{18}	3.6×10^{18}	5.4×10^{18}	8.1×10^{18}
Steady-state density of buffer gas atoms, $\text{mol} \cdot \text{cm}^3$	4.9×10^{13}	1.9×10^{14}	3.9×10^{14}	5.8×10^{14}	8.8×10^{14}
Diffusion time, ms**	0.5	2.2	4.6	6.8	10.4

Table 1. Summary of flow rate dependence on diffusion time for 1 micron, 1 cm^2 glycolaldehyde ice sample with $4 \times 10^{15} \text{ mol s}^{-1}$ coming off of the ice, a corresponding number density of $4.2 \times 10^{11} \text{ mol} \cdot \text{cm}^{-3}$ of the molecules of interest within the 100 cm^2 cell which has a 3 cm^2 aperture, and 9.2 L s^{-1} conductance. ** The molecule to be cooled is 60 amu and has a collisional cross section with neon at 20 K of $2.4 \times 10^{-15} \text{ cm}^2$ (see Ref 15).

A number density of $1.9 \times 10^{14} \text{ cm}^{-3}$ buffer gas atoms (the steady-state condition at a 4 sccm flow rate) at 20 K yields a pressure of 3.8×10^{-4} torr within the cell. The performance curves reported for an Osaka TG2400M (2400 L/s) magnetically levitated turbo pump indicate that in the chamber, a pressure of 2×10^{-5} torr can be achieved with a 4 sccm flow rate of N_2 or Ar, with similar performance expected for neon. While cryo pumps are extremely effective, they must be emptied periodically and have reduced pumping speeds as they begin to fill[31,32].

IV. Spectrometer Sensitivity

In order to ensure chirped-pulse mmWave spectroscopy has sufficient sensitivity to operate under the conditions outlined above, we have examined the performance of a similar spectrometer applied to interrogate molecules at 10 – 20 K in a sampled uniform Laval flow (CPUF[33,34]) and the results are presented here. 0.3% OCS (99% purity, Metro Welding Supply Corp.) in N₂ carrier gas was studied under conditions in which the rotational temperature at the probe region was determined to be 14.7 K (established using a number of rotational lines of propionitrile) and the total number density was $\sim 2.1 \times 10^{14} \text{ mol} \cdot \text{cm}^{-3}$. The J = 7 – 6 transition at 83.057 GHz of the OC³⁴S isotopologue with a natural abundance of 4.2% (corresponding to a number density of $2.7 \times 10^{10} \text{ mol} \cdot \text{cm}^{-3}$) was probed with a 200 MHz chirp. Under broadband (fast passage) conditions, the signal-to-noise ratio (S/N) was determined to be 25:1 after 200,000 acquisitions at a repetition rate of 5 Hz with 30 acquisitions per gas pulse. In broadband rotational spectroscopy, the factors that govern the signal intensity are summarized by equation 4[6],

$$S \propto \omega \mu_{ij}^2 E \Delta N_0 \alpha^{-1/2} \quad \text{Eq. 4}$$

where ω is the frequency of the rotational transition of interest, μ_{ij} is the transition dipole moment, E is the electric field strength of the pulse, ΔN_0 is the population difference between the two adjacent rotational states of interest, and α is the linear sweep rate of the chirp. Although we have broadband capability, the highest sensitivity may be achieved with a $\pi/2$ pulse. The J = 7 – 6 transition of OC³⁴S was probed under the same conditions described above with a $\pi/2$ pulse in which the maximum polarization is achieved at 1397 ns, corresponding to an electric field strength of 68 V/m. In this case the S/N obtained after 200,000 averages was 45:1. The relative intensities observed under each condition are shown in Figure 2.

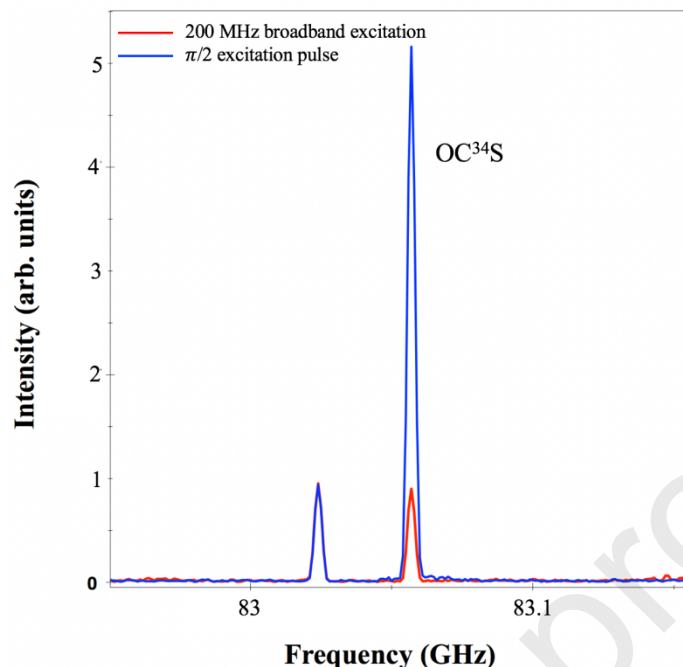


Figure 2. $J = 7 - 6$ transition of OC^{34}S probed with both a 200 MHz (red trace) and $\pi/2$ pulse (blue trace). The lower-frequency peak present in both spectra is an artifact from noise in the electronics and not valve-dependent.

On the basis of these findings, the sensitivity of the CPUF spectrometer is clearly adequate for detection of buffer gas cooled molecules that have sublimed from an ice substrate. We now examine factors that can be optimized to enhance the S/N of the proposed instrument. The CPUF instrument is pulsed and permitted 60 acquisitions $\cdot \text{sec}^{-1}$. Considering the continuous operation of the buffer gas cell within which cooled molecules will be detected in the proposed work, high repetition rates may be employed[22]. At 50k shots $\cdot \text{sec}^{-1}$, over the course of a 5 minute TPD period, 15 million shots will be acquired. Extrapolating from the performance reported for the above experiment under the $\pi/2$ condition and assuming Poisson noise, a S/N ratio of 390:1 can be expected at a number density of $2.7 \times 10^{10} \text{ mol} \cdot \text{cm}^{-3}$. Again extrapolating from the measured conditions, we find a detection limit of $3.1 \times 10^9 \text{ mol} \cdot \text{cm}^{-3}$, defined as that giving a S/N of 5. The corresponding values for the broadband scan are a S/N of 216:1 and detection limit of $4.1 \times 10^9 \text{ mol} \cdot \text{cm}^{-3}$. We note this detection limit corresponds to the thermal ensemble of molecules, not those in a particular quantum state. Moreover, this assumes the same probe volume in the cell and the sampled flow; the latter volume is difficult to estimate in the present case but is

likely at least three times smaller than that in the cell, suggesting that these relative signals represent a conservative estimate.

	OC ³⁴ S, 15 K	GA, 15 K	Factor v OCS	GA, 200 K	Factor v 15K GA	DME, 15 K	Factor v OCS	DME, 200K	Factor v 15 K DME
Frequency, GHz	83.057	75.277	0.9	75.277	1	82.650	0.995	82.650	1
μ_{ij}^{2*}	3.6	32.4	9.1	32.4	1	54.7	15.3	54.7	1
ΔN , mol · cm ⁻³	1.2 x 10 ⁸	4.6 x 10 ⁹	38.3	2.6 x 10 ⁶	5.7 x 10 ⁻⁴	1.2 x 10 ¹⁰	100	1 x 10 ⁸	8.3 x 10 ⁻³
Relative Signal, Broadband	1	-	314	-	0.0006	-	152	-	0.008
Detection Limit, Broadband	4.1 x 10 ⁹	1.3 x 10⁷	-	2.3 x 10¹⁰	-	2.7 x 10⁶	-	3.2 x 10⁸	-

Table 2. Summary of computed signal intensities in comparison with the OC³⁴S data obtained in the CPUF spectrometer. The $E_{pulse} = 68$ V/m with a sweep rate α of 1 GHz/ μ s was used for this comparison. *From the Cologne Database of Molecular Spectroscopy, refs 38 and 39.

It is useful to compare the signal intensities we expect from molecules of interest in the proposed experiment where one chief aim will be to understand pathways to molecular complexity in the interstellar medium. As such, we consider the $J = 10 - 9$ transition of glyoxylic acid (GA) and the $J = 3 - 2$ transition of dimethyl ether (DME), both candidates that we will initially target in future studies and both more favorable species for detection in the 60 – 90 GHz region than OCS. Table 4 summarizes the computed signal strengths for these molecules following buffer gas cooling in comparison with the OCS $J = 7 - 6$ transition measured here at 14.7 K under broadband and $\pi/2$ conditions. The number density of molecules used to determine ΔN_0 at 20 K are based on the TPD measurements from Kaiser et al, in which GA and DME desorb between 200 – 230 K and 100 – 115 K, respectively[35,36]. On the basis of Equation 3 for broadband signal intensity and the expression from McGurk et al. (Eq 56 from Ref 37) relating this to the $\pi/2$ condition[37], we expect significantly stronger signal intensities and better S/N in the proposed experiment in comparison with that presented in Fig 2 (a factor of 11 for GA and 4 for DME with a 1 GHz/ μ s sweep rate). This is in part related to the much larger population difference in the 60 - 90 GHz regime for these molecules in comparison with OCS, and in part

due to their larger dipole moments[38,39]. Also included in Table 4 is a comparison of the signal intensity for these species for detection at their corresponding sublimation temperatures where intensities are weaker by orders of magnitude as a result.

V. Conclusion

Broadband rotational spectroscopy has been widely applied in creative ways to understand the structure and dynamics of molecules[40-44]. A natural, but largely unexplored application of this approach is to understand the chemistry of molecules generated in ice. Buffer gas cooling will enable such investigations, allowing new insight into important origin-of-life questions. For example, it has been proposed that interstellar ice photochemistry may be the source of enantiomeric excess on the nascent earth[2]. The conditions under which this occurs and to what extent is not yet known, in large part due to experimental limitations. Exotic approaches such as chiral sensing have been made possible by microwave three-wave mixing, a direct way in which to gain insight into the question of enantiomeric excess[45-47]. The proposed instrument is not limited to investigations of interstellar or cometary ice chemistry. Additional applications include the synthesis of exotic molecules such as those generated by Kaiser et al[48], in which ices lend themselves to the generation of unstable species not practically synthesized in the gas-phase. The simultaneous high resolution and broadband nature of chirped pulse Fourier Transform mmWave spectroscopy has made possible the structural characterization of large, complex molecules making this a promising and interesting application of the technique.

Acknowledgements

This work was supported by the University of Missouri, Department of Chemistry start-up funds. We wish to thank Dave Patterson and Lincoln Satterthwaite for their generous insights into buffer gas cooling. We also thank Ralf Kaiser for his thoughtful advice on the UHV ice instrument design. Finally, we thank Arthur Suits for helpful discussions.

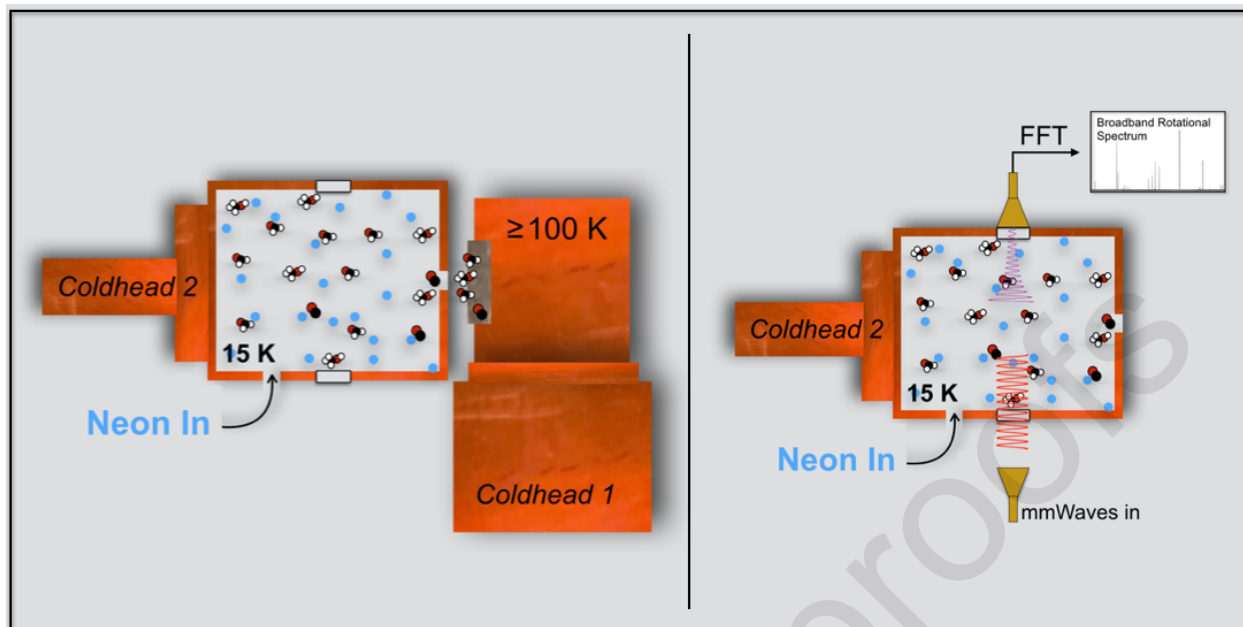
Journal Pre-proofs

References

- [1] E.F. Van Dishoeck, *Faraday Discussions* 168 (2014) 9.
- [2] K.I. Öberg, *Chemical Reviews* 116 (2016) 9631.
- [3] M. Nuevo, U. Meierhenrich, L. d'Hendecourt, G.M. Caro, E. Dartois, D. Deboffle, W.-P. Thiemann, J.-H. Bredehöft, L. Nahon, *Advances in Space Research* 39 (2007) 400.
- [4] C. Meinert, I. Myrgorodska, P. De Marcellus, T. Buhse, L. Nahon, S.V. Hoffmann, L.L.S. d'Hendecourt, U.J. Meierhenrich, *Science* 352 (2016) 208.
- [5] G.B. Park, R.W. Field, *The Journal of Chemical Physics* 144 (2016) 200901.
- [6] G.G. Brown, B.C. Dian, K.O. Douglass, S.M. Geyer, S.T. Shipman, B.H. Pate, *Review of Scientific Instruments* 79 (2008) 053103.
- [7] K.M. Yocum, H.H. Smith, E.W. Todd, L. Mora, P.A. Gerakines, S.N. Milam, S.L. Widicus Weaver, *The Journal of Physical Chemistry A* 123 (2019) 8702.
- [8] P. Theulé, C. Endres, M. Hermanns, J.-B. Bossa, A. Potapov, *ACS Earth and Space Chemistry* 4 (2019) 86.
- [9] D. Patterson, J.M. Doyle, *Molecular Physics* 110 (2012) 1757.
- [10] N.R. Hutzler, H.-I. Lu, J.M. Doyle, *Chemical Reviews* 112 (2012) 4803.
- [11] D. Patterson, E. Tsikata, J.M. Doyle, *Physical Chemistry Chemical Physics* 12 (2010) 9736.
- [12] D. Egorov, W. Campbell, B. Friedrich, S. Maxwell, E. Tsikata, L. Van Buuren, J. Doyle, *The European Physical Journal D-Atomic, Molecular, Optical and Plasma Physics* 31 (2004) 307.
- [13] D. Egorov, T. Lahaye, W. Schöllkopf, B. Friedrich, J.M. Doyle, *Physical Review A* 66 (2002) 043401.
- [14] Y. Zhou, D.D. Grimes, T.J. Barnum, D. Patterson, S.L. Coy, E. Klein, J.S. Muentzer, R.W. Field, *Chemical Physics Letters* 640 (2015) 124.
- [15] M.J. Abplanalp, R.I. Kaiser, *Physical Chemistry Chemical Physics* 21 (2019) 16949.
- [16] R. Martín-Doménech, K.I. Öberg, M. Rajappan, *The Astrophysical Journal* 894 (2020) 98.
- [17] T. Gantner, M. Koller, X. Wu, G. Rempe, M. Zeppenfeld, *Journal of Physics B: Atomic, Molecular and Optical Physics* (2020).

- [18] W.C. Campbell, J.M. Doyle, *Cold Molecules: Theory, Experiment, Applications* (2009) 473.
- [19] J. Messer, F.C. De Lucia, *Physical Review Letters* 53 (1984) 2555.
- [20] S. Eibenberger, J. Doyle, D. Patterson, *Physical Review Letters* 118 (2017) 123002.
- [21] J.P. Porterfield, L. Satterthwaite, S. Eibenberger, D. Patterson, M.C. McCarthy, *Review of Scientific Instruments* 90 (2019) 053104.
- [22] J.P. Porterfield, S. Eibenberger, D. Patterson, M.C. McCarthy, *Physical Chemistry Chemical Physics* 20 (2018) 16828.
- [23] N. Tariq, N. Al Taisan, V. Singh, J.D. Weinstein, *Physical Review Letters* 110 (2013) 153201.
- [24] P.B. Changala, M.L. Weichman, K.F. Lee, M.E. Fermann, J. Ye, *Science* 363 (2019) 49.
- [25] B.M. Jones, R.I. Kaiser, *The Journal of Physical Chemistry Letters* 4 (2013) 1965.
- [26] L. Satterthwaite, C. Pérez, A.L. Steber, D. Finestone, R.L. Broadrup, D. Patterson, *The Journal of Physical Chemistry A* 123 (2019) 3194.
- [27] J.P. Porterfield, J. Westerfield, L. Satterthwaite, D. Patterson, P.B. Changala, J.H. Baraban, M.C. McCarthy, *The Journal of Physical Chemistry Letters* 10 (2019) 1981.
- [28] D. Patterson, J. Rasmussen, J.M. Doyle, *New Journal of Physics* 11 (2009) 055018.
- [29] K.S. Twyman, M.T. Bell, B.R. Heazlewood, T.P. Softley, *The Journal of Chemical Physics* 141 (2014) 024308.
- [30] J.M. Hollis, F.J. Lovas, P.R. Jewell, *The Astrophysical Journal Letters* 540 (2000) L107.
- [31] J. Barry, E. Shuman, D. DeMille, *Physical Chemistry Chemical Physics* 13 (2011) 18936.
- [32] N.R. Hutzler, M.F. Parsons, Y.V. Gurevich, P.W. Hess, E. Petrik, B. Spaun, A.C. Vutha, D. DeMille, G. Gabrielse, J.M. Doyle, *Physical Chemistry Chemical Physics* 13 (2011) 18976.
- [33] J.M. Oldham, C. Abeysekera, B. Joalland, L.N. Zack, K. Prozument, I.R. Sims, G.B. Park, R.W. Field, A.G. Suits, *The Journal of Chemical Physics* 141 (2014) 154202.
- [34] C. Abeysekera, L.N. Zack, G.B. Park, B. Joalland, J.M. Oldham, K. Prozument, N.M. Ariyasingha, I.R. Sims, R.W. Field, A.G. Suits, *The Journal of Chemical Physics* 141 (2014) 214203.
- [35] A.K. Eckhardt, A. Bergantini, S.K. Singh, P.R. Schreiner, R.I. Kaiser, *Angewandte Chemie International Edition* 58 (2019) 5663.

- [36] A. Bergantini, S. Góbi, M.J. Abplanalp, R.I. Kaiser, *The Astrophysical Journal* 852 (2018) 70.
- [37] J. McGurk, T. Schmalz, W. Flygare, *The Journal of Chemical Physics* 60 (1974) 4181.
- [38] H.S. Müller, S. Thorwirth, D. Roth, G. Winnewisser, *Astronomy & Astrophysics* 370 (2001) L49.
- [39] H.S. Müller, F. Schlöder, J. Stutzki, G. Winnewisser, *Journal of Molecular Structure* 742 (2005) 215.
- [40] K. Prozument, J.H. Baraban, P.B. Changala, G.B. Park, R.G. Shaver, J.S. Muentzer, S.J. Klippenstein, V.Y. Chernyak, R.W. Field, *Proceedings of the National Academy of Sciences* 117 (2020) 146.
- [41] B.C. Dian, G.G. Brown, K.O. Douglass, B.H. Pate, *Science* 320 (2008) 924.
- [42] N.M. Kidwell, V. Vaquero-Vara, T.K. Ormond, G.T. Buckingham, D. Zhang, D.N. Mehta-Hurt, L. McCaslin, M.R. Nimlos, J.W. Daily, B.C. Dian, *The Journal of Physical Chemistry Letters* 5 (2014) 2201.
- [43] K. Prozument, A.P. Colombo, Y. Zhou, G.B. Park, V.S. Petrović, S.L. Coy, R.W. Field, *Physical Review Letters* 107 (2011) 143001.
- [44] N. Dias, B. Joalland, N.M. Ariyasingha, A.G. Suits, B.M. Broderick, *The Journal of Physical Chemistry A* 122 (2018) 7523.
- [45] D. Patterson, M. Schnell, J.M. Doyle, *Nature* 497 (2013) 475.
- [46] V.A. Shubert, D. Schmitz, D. Patterson, J.M. Doyle, M. Schnell, *Angewandte Chemie International Edition* 53 (2014) 1152.
- [47] D. Patterson, M. Schnell, *Physical Chemistry Chemical Physics* 16 (2014) 11114.
- [48] G. Tarczay, M. Förstel, S. Góbi, P. Maksyutenko, R.I. Kaiser, *ChemPhysChem* 18 (2017) 882.



Highlights

- Chemistry taking place in ice is an important component of interstellar and atmospheric chemistry
- Broadband rotational spectroscopy has not yet been applied to interrogate this chemistry due to the high temperatures at which organic molecules enter the gas phase
- The proposed technique employs buffer gas cooling to allow for the application of rotational spectroscopic probes of interstellar or cometary ices

Credit Author Statement

CPLETT-20-1781

Bernadette Broderick: Conceptualization, Methodology, Investigation, Writing – Original draft preparation

Ranil Gurusinge: Investigation, Writing – Reviewing and editing

Nureshan Dias: Investigation

Journal Pre-proofs

Declaration of interests

The authors declare that they have no known competing financial interests or personal relationships that could have appeared to influence the work reported in this paper.

The authors declare the following financial interests/personal relationships which may be considered as potential competing interests: